Journal of Nano- and Electronic Physics
Vol. **12** No 2, 02042(4pp) (2020)

Журнал нано- та електронної фізики
Том **12** № 2, 02042(4cc) (2020)

Fabrication of Roughness Enhanced Hydrophobic Coatings

J. Shanthi*, Aishwarya S., Swathi R.

Department of Physics, Avinashilingam Institute for Home-science and Higher Education for Women, Coimbatore, India

(Received 12 February 2020; revised manuscript received 10 April 2020; published online 25 April 2020)

The non-wetting character derived with the lotus-leaf phenomenon of water droplet rolling off from leaf indicates the Hydrophobic/Super-hydrophobic surface which depends on the morphology and the topography of surfaces, described by the Wenzel and Cassie–Baxter theories. Hydrophobicity arises when a molecule does not partake in the hydrogen bonding of water. The water droplet is suspended on a composite interface made of solid and air trapped between the droplet and the surface. Materials with superhydrophobic or superoleophobic properties are in extreme demand due to numerous potential applications such as in anti-corrosion coatings, self-cleaning, anti-icing coatings, liquid-repellent textiles, oil/water separation, microfluidic devices, optical devices. Films of PVDF/MTMS and PVDF/MTMS/TEOS were prepared by sol-gel technique. PVDF/MTMS and PVDF/MTMS/TEOS film shows a surface roughness of 60.76 μm and 57.64 μm with contact angle 132° and 125° respectively, which ensures hydrophobicity. The film developed was found to be super-hydrophobic and could remove the dust on coated glass, metallic surfaces and hence can be assured for Self-cleaning application.

Keywords: Superhydrophobic, Surface roughness, PVDF/MTMS, Non-wetting character.

DOI: 10.21272/jnep.12(2).02042 PACS number: 81.15. – z

1. INTRODUCTION

Nature is a wide source of advanced research and techniques. So it is necessary to learn from nature for better ideas. The concept of hydrophobicity is one of such idea, inspired from lotus leaf. Variety of man-made approaches has been followed to mimic those surfaces to create artificial hydrophobic surfaces [1]. Hydrophobic surfaces exhibit water-repellent properties which have both scientific and industrial interest, because of their wide range of applications, such as oil-water separation, self-cleaning, anti- icing etc [2, 3]. The cause of self- cleaning properties of the lotus leaf is the hydrophobic water repellent double structure of the surface. This enables the contact area and the adhesion force between surface and droplet to be significantly reduced and results in a self- cleaning process allowing water to readily roll off the leaf and collect dust deposits on the way [4]. The naturally occurring hydrophobic surfaces achieve the high contact angle values because of the rough surfaces coated with the low surface energy wax, which has high repelling interactions with the polar solvents including water. Hannuteislaet al., and Harinarayanan et al., have reported innumerable methods to fabricate hydrophobic coatings. The methods include dip-coating, spray-coating, sol-gel method, spin coating, hydrothermal synthesis, plasma etching. Low surface energy is the salient feature for hydrophobic surfaces. Silica coatings obtained from the sol-gel method and spincoating technique have genuinty as reported by cristianpetcu et al. Production of hydrophobic coatings has been developed by different surface modification methods such as dip-coating, spray- coating, sol-gel method, spin coatingetc.Here in this work we reported self-cleaning behavior of composite films.

2. MATERIALS & METHOD

2.1 Materials

Reagent-grade Methyltrimethoxysilane (MTMS) and Tetraethoxysilane (TEOS) and a highly non reactive Thermoplastic fluoropolymerPolyvinylidenefluoride (PVDF, 275000-MW) obtained from Sigma Aldrich. PVDF is mainly used in critical applications requirng an excellent chemical resistance, high degree of purity, high dielectric response and good mechanical properties.Ethanol-absolute grade (100% purity) waspurchased from Hayman and HCl AR grade, DMF were purchased from meck.

2.2 Sample Preparation

The PVDF/MTMS composite has been prepared with PVDF and MTMS. The PVDF solution was prepared by adding 1 g of PVDF with 15 ml of DMF, which was stirred for one hour at 30 °C in magnetic stirrer to get homogeneous solution. 0.2 ml of MTMS was mixed with 2 ml of ethanol, stirred for 30 minutes. The PVDF and MTMS sols were intermixed and the obtained solution was kept in water bath for 30 minutes to yield uniformity. The prepared sol was kept for aging at room temperature for two hours.

The PVDF/MTMS/TEOS composite has been prepared with TEOS, MTMS and PVDF. Initially the polymer sol was prepared separately. 0.5 g of PVDF was dissolved in 10 ml of DMF using sonication for 45 minutes. After that 0.2 ml of TEOS and 0.1ML of MTMS were added drop-wise to the polymer sol and sonicated for 15 minutes to get homogeneous solution.

The obtained sol was aged for 10 hours and coated on a clean glass substrate using spin coating unit with 1200 rpm speed for 120 sec. The coated glass substrate was then annealed in a muffle furnace at 100°C with minimum degree of ramping rate.

*shanthinelson@gmail.com

 © 2020 Sumy State University

3. CHARACTERIZATION

The PVDF/MTMS and PVDF/MTMS/TEOS composite films were characterized. The presence of various functional groups has been identified by fourier-transform infrared spectroscopy. With 3*D* laser zeta profilometry the roughness of surface was analysed. Field emission scanning electron microscope reveals the surface morphology of the coated film. Surface morphology of the prepared samples were identified using contact angle measurement.

4. RESULT AND DISCUSSION

4.1 FTIR Analysis

The FTIR spectra reveal the presence of functional groups in PVDF/MTMS and PVDF/TEOS/MTMS composite films. Pristine PVDF shows standard absorption peaks at 610,759,796 cm^{-1} attribute non-polar α-phase. While the presence of FTIR peak at 835 cm^{-1} indicates the γ-phase [7]. From Fig. 1 the two characteristic peaks of PVDF at 1400 and 1175 cm^{-1} attributed to the CH_2 and CF_2 stretching vibration respectively [9]. The characteristic bands appeared at 835, 871, 1062 cm^{-1} of pristine PVDF changes into 831, 874, 1068 cm^{-1} for blend which shows the presence of MTMS. The peak appeared at 1400 cm^{-1} of pristine PVDF is also present in the blend hence the presence of PVDF. The peaks at 3022, 3611 cm^{-1} indicates the absence of water molecule which ensures the hydrophobic nature.

From the Fig. 2 the peak at 767 cm^{-1} and 832 cm^{-1} refers to the non- polar α-phase and γ-phase of PVDF seen in TEOS/MTMS/PVDF film [8].The peak at 1400 cm^{-1} and 1165 cm^{-1} shows CH_2 and CF_2 stretching vibration [9].With the presence of silane, Si-O-Si stretching has been deformed to linear structure. Beyond, 3000 cm^{-1}, absence of polar bond is observed.

4.2 Thermal Analysis

TG/DTA for PVDF/MTMS and PVDF/MTMS/TEOS was shown in Figs. 3 and 4. An Initial weight loss about 65ºC shown in fig 4 is mainly due to solvent evaporation. Major weight loss was observed in range 400-500 °C for the prepared sample. This could correspond to structural decomposition of the polymer blend and their complexes. The sample is stable upto 520 °C.

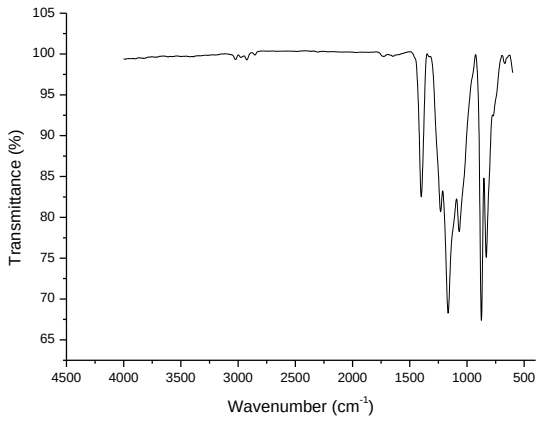

Fig. 1 – FTIR Spectra of PVDF/MTMS blend film

A sharp and large exothermic peak appeared at 490 °C concurrent with a considerable weight loss of about 74.73 % and this indicate the complex decomposition of the film, which is in agreement with the TG curve. From the above discussion, it is clear that the film has good thermal stability upto 460 ºC [10]. Figure 4 represents single stage decomposition, with an exothermic peak at 480 °C and the weight loss was about 76.23%, which is due to the volatile and polymeric materials.

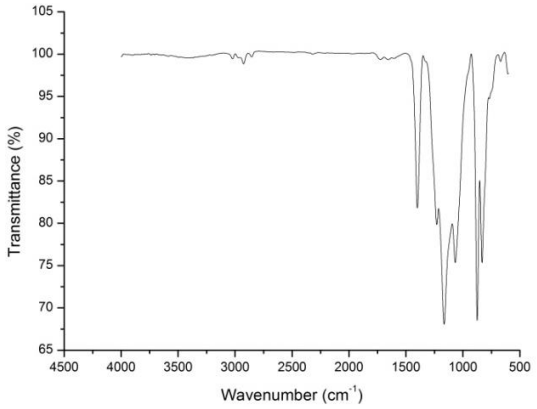

Fig. 2-FTIR spectra of PVDF/MTMS/TEOS blend film

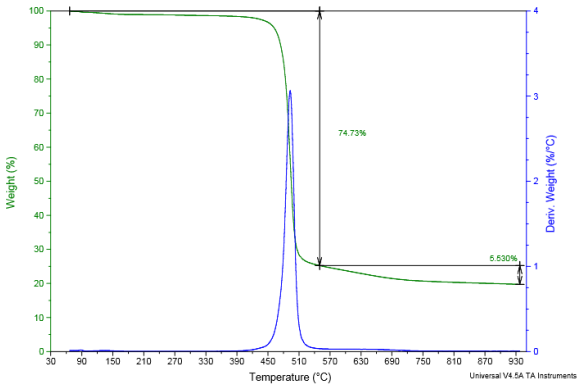

Fig. 3 – TG/DTA curve of PVDF/MTMS film

4.3 FE-SEM

Microstructure images of the membrane surfaces were obtained using a scanning electron microscope. Fig 5 shows the FE-SEM analysis of the PVDF/MTMS composite film. The film which shows appropriate surface roughness due to the presence of micro sized particles. With the addition of MTMS more and more microspheres were observed on the surface. These have an important role, to make the surface non-wettable [11]. TEOS/MTMS/PVDF morphology is shown in the Fig. 6 which implements rough surface. Such surface formation hold good for hydrophobicity.

4.4 Surface Roughness and Energy

The surface roughness of the films PVDF/MTMS and PVDF/MTMS/TEOS were analyzed using 3*D* Laser profilometry and the roughness was found to be 60.76 μm and 57.64 μm respectively. Higher the surface roughness, higher will be the contact angle with reduction in surface energy [12, 13]. Surface energy caused

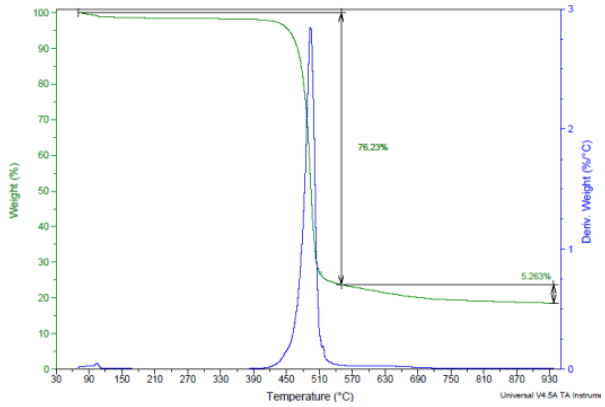

Fig. 4 – TG/DTA curve of PVDF/MTMS/TEOS film

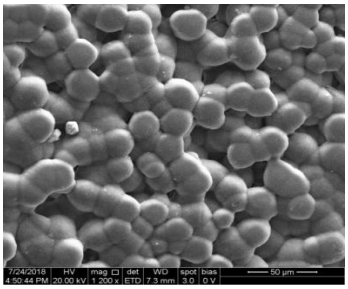

Fig. 5 – FE-SEM image of PVDF/MTMS

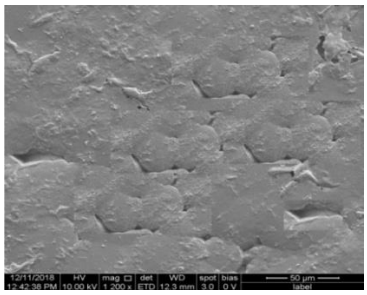

Fig. 6 – FE-SEM image of PVDF/MTMS/TEOS

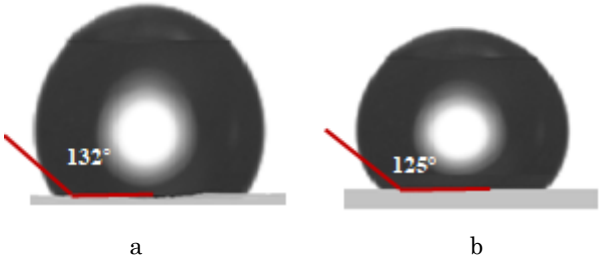

a b

Fig 7 – (a) Contact Angle of PVDF/MTMS (b) Contact Angle of PVDF/MTMS/TEOS

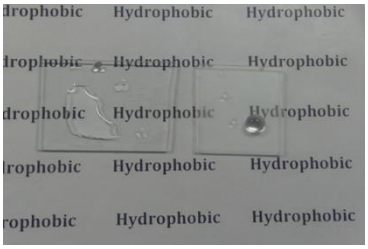

Fig. 8 – Water droplets on (a) Uncoated substrate and (b) Coated substrate

by intermolecular interactions at the interface may be same kind or different. Surface energy of polymers can be measured based on wettability [14]. Lift shifts theory of vander waals interaction successively explains the interaction of uncharged macroscopic surfaces across air or water [15]. Surface energy can be effectively calculated by using Hamakers constants, which was discussed earlier by [16, 17]. The computed surface energy values are tabulated in Table 1 and the histogram representing the particle size was plotted in Fig. 9 (c) and (d).

The blend film was found to be hydrophobically effective in many applications such as self-cleaning, anti-dust, and even as water proof material. Figs. 10 (a) and (b) representing the photographs of uncoated and

Table 1 – Calculated values of Surface free energy

Polymer blend	Hamaker Constant An ($J \cdot 10^{-21}$)	Surface free energy γ, ($J \cdot m^{-1}$)	Contact Angle (CA) (°)
PVDF/MTMS	1.16	41.2	132°
PVDF/MTMS/TEOS	2.086	17.49	125°

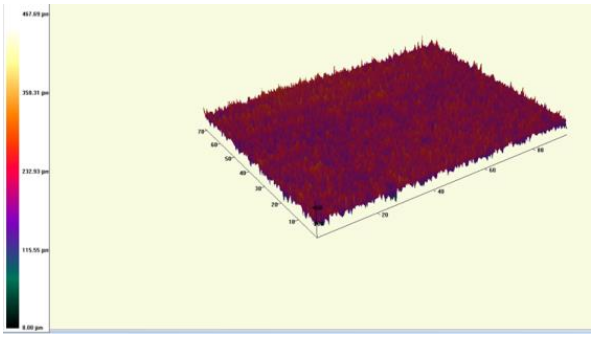

a

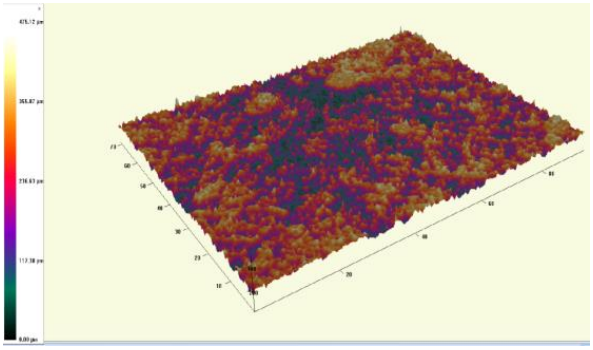

b

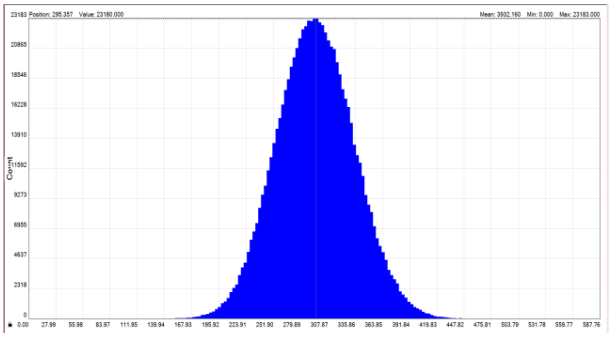

c

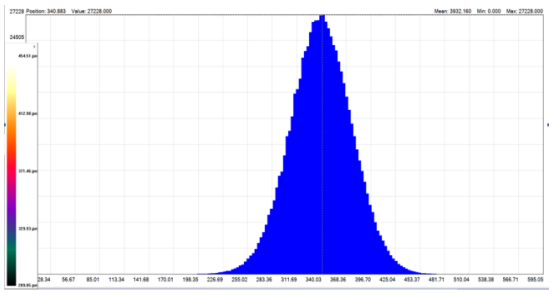

d

Fig. 9 – (a) Surface roughness of PVDF/MTMS and (b) surface roughness of PVDF/MTMS/TEOS; (c) histogram of PVDF/MTMS and (d) histogram of PVDF/MTMS/TEOS

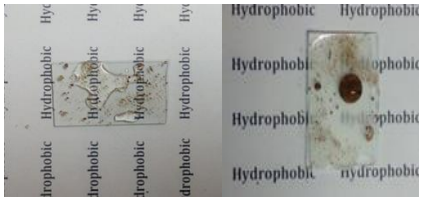

a b

Fig. 10 – (a) Uncoated glass substrate with the dust particles and (b) PVDF/MTMS coated glass substrates with the dust particles clinged together to the water droplet-ensures the self-cleaning property

coated substrates. The coated substrates were exposed to dust for about three hours, later, water was allowed on the substrates, which resulted in rolling-off the water from the surface along with the dust. This proves that the PVDF/MTMS blend coated films has the ability to remove the dust due to its self-cleaning property. Fig. 10 (b) shows the water roll-off along with the dust.

5. CONCLUSION

PVDF/MTMS and PVDF/MTMS/TEOS blend films was successfully obtained by sol-gel technique. The fluoride based polymer incorporated with silane, proved to have non-wetting property as the film possess higher contact angle and surface roughness. The thermal studies prove the thermal stability of the film upto 520 °C. The films found to be applicable in self-cleaning, anti-corrosive, and water-proof textile.

ACKNOWLEDGEMENT

We acknowledge Polymer science department, Central Leather Research Institute, Adyar for providing Contact angle measurement facility and Indian Institute of Technology (IIT), Chennai for Thermal analysis. This research did not receive any specific grant from funding agencies in the public, commercial, or not-for-profit sectors.

REFERENCES

1. Nan Wang, Yao Lu, Dangsheng Xiong, Claire J. Carmalt Ivan, P. Parkin, *J. Mater. Chemi A* **4**, 4107 (2016).
2. Leila Shams Solaree, Ahmad Monshi, Hamid Ghayour, *Synth. React. Inorg. Metal-Organic, Nano-Metal Chem.* **45**, 1769 (2015).
3. Nils O. Petersen, *Foundations for Nanoscience and Nanotechnolog,* 360 (CRC Press: 2017).
4. Lin Feng, Shuhong Li, Yingshun Li, Huanjun Li, Lingjuan Zhang, Lei jiang, *Adv. Mater.* **14**, 1857 (2002).
5. Hannu Teisala, Mikko Tuominen, Jurkka Kuusipalo, *Adv. Mater. Interfaces* **1**, 1300026 (2014).
6. Harinarayanan Puliyalil, Gregor Filipic, Uros Cvelbar, *Intech* **311**, (2015).
7. Cristian Petcu, Cristina Lavinia Nistor, Violeta Purcar, Ludmila Otilia Cinteza, Catalin-Illie Spataru, Marius Ghiurea, Raluca Lanchis, Mihai Anastasescu, *Appl. Surf. Sci.* **347**, 359 (2015).
8. Vimal K. Tiwari, Yujeong Lee, Giyoung Song, Kang Lib Kim, Youn Jung Park, Cheolmin Park, *Polymer Sci.* **56**, 795 (2018).
9. Hossein Mahdavi, Akram Rahimi, Leila Ahmaadian Alam, *Polymer Bull.* **74**, 3557 (2017).
10. Binny Krishnankutty, Shantala Bellary, BR Naveen Kumar, Latha S Moodahadu, *IJP* **44(5)**, 168 (2012).
11. Zhenxing Wang, ShengqiangJi, Fang He, Moyuan Cao, ShaoqinPeng, Yuexiang Li, *J. Mater. Chem. A* **6**, 3391 (2018).
12. S.G. Deshmukh, A.K. Panchal, Vipul Kheraj, *J. Mater. Sci.: Mater. Electron.* **28**, 11926 (2017).
13. S.G. Deshmukh, Vipul Kheraj, K.J. Karande, R.S. Deshmukh, *Mater. Res. Express* **6**, 084013 (2019).
14. Soo-Jin Park, Min-Kang Seo, *Interface Sci. Technol.* **18**, 59 (2011).
15. Calcum J. Drummond, Derek Y.C. Chan, *Langmuir* **13**, 3890 (1997).
16. J. Vial, A. Carre, *Int. J. Adhes. Adhes* **11**,140 (1991).
17. J. Shanthi, S. Aishwarya, R. Swathi, *Mater. Let.* **253**, 409 (2019).